

NUWC-NPT Technical Report 10,338
1 September 1994

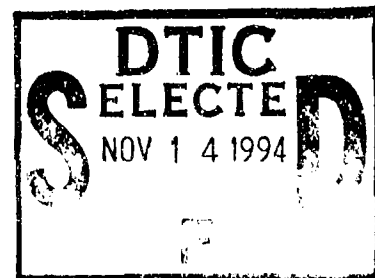
AD-A286 080



48
11

A Vehicle Trajectory Method for Intercepting an Alerted, Evading Contact

A. F. Bessacini
R. F. Pinkos
Combat Control Systems Department



328
94-35057
424487



Naval Undersea Warfare Center Division
Newport, Rhode Island

Approved for public release; distribution is unlimited.

DTIC QUALITY INSPECTED 5

PREFACE

This report was prepared under the Naval Undersea Warfare Center Division, Newport, RI, Bid and Proposal (B&P) Program. The B&P program provides funding for preliminary, conceptual, and technical work necessary for the generation of complete and comprehensive proposals for direct-funded work.

The technical reviewer for this report was A. H. Silva (Code 22101).

Reviewed and Approved: 1 September 1994

A handwritten signature in cursive script, appearing to read "P. A. La Brecque".

P. A. La Brecque
Head, Combat Control Systems Department

REPORT DOCUMENTATION PAGE

Form Approved
OMB No. 0704-0188

Public reporting for this collection of information is estimated to average 1 hour per response, including the time for reviewing instructions, searching existing data sources, gathering and maintaining the data needed, and completing and reviewing the collection of information. Send comments regarding this burden estimate or any other aspect of this collection of information, including suggestions for reducing this burden, to Washington Headquarters Services, Directorate for Information Operations and Reports, 1215 Jefferson Davis Highway, Suite 1204, Arlington, VA 22202-4302, and to the Office of Management and Budget, Paperwork Reduction Project (0704-0188), Washington, DC 20503.

1. AGENCY USE ONLY (Leave blank)		2. REPORT DATE 1 September 1994	3. REPORT TYPE AND DATES COVERED Final	
4. TITLE AND SUBTITLE A Vehicle Trajectory Method for Intercepting an Alerted, Evading Contact			6. FUNDING NUMBERS	
6. AUTHOR(S) A. F. Bessacini R. F. Pirkos				
7. PERFORMING ORGANIZATION NAME(S) AND ADDRESS(ES) Naval Undersea Warfare Center Division 1178 Howell Street Newport, Rhode Island 02841-1708			8. PERFORMING ORGANIZATION REPORT NUMBER TR 10,338	
9. SPONSORING/MONITORING AGENCY NAME(S) AND ADDRESS(ES)			10. SPONSORING/MONITORING AGENCY REPORT NUMBER	
11. SUPPLEMENTARY NOTES				
12a. DISTRIBUTION/AVAILABILITY STATEMENT Approved for public release; distribution is unlimited.			12b. DISTRIBUTION CODE	
13. ABSTRACT (Maximum 200 words) This report deals with the determination of a vehicle trajectory that will result in intercept of an alerted, evading contact. One of the classical problems associated with vehicle employment is the calculation of those parameters necessary for a vehicle trajectory to result in either intercept of a contact or for the vehicle to be delivered to a location that is suitable for the internal seeker system of the vehicle to detect and home on the contact. The primary parameters associated with such a problem are: vehicle deflection or gyro angle, intercept time, and seeker turn-on time. This study extends existing work by formulating a method and solving the associated equations that allow for the treatment of an alerted contact when the contact's sensor detection capability, along with an evasion strategy, is postulated. A computer simulation is used to verify performance.				
14. SUBJECT TERMS Intercept Trajectories Combat Control Systems Evasion Weapon, Order Generation Pursuer/Evader			15. NUMBER OF PAGES 31	
			16. PRICE CODE	
17. SECURITY CLASSIFICATION OF REPORT Unclassified	18. SECURITY CLASSIFICATION OF THIS PAGE Unclassified	19. SECURITY CLASSIFICATION OF ABSTRACT Unclassified	20. LIMITATION OF ABSTRACT SAR	

TABLE OF CONTENTS

Section	Page
LIST OF TABLES	ii
LIST OF SYMBOLS	ii
1 INTRODUCTION.....	1
2 PROBLEM DEFINITION.....	3
3 FORMULATION/SOLUTION OF EQUATIONS.....	5
Formulation of Equations.....	5
Solution of Equations	13
4 RESULTS	19
5 CONCLUSIONS	27
6 REFERENCES.....	29

LIST OF ILLUSTRATIONS

Figure	Page
1 Overall Block Diagram of System	5
2 Functional Block Diagram of the Evading Contact Intercept Computational Unit.....	6
3 Geometry Depicting Various Points in Vehicle Trajectories.....	7
4a Contact Track.....	8
4b Pursuer Track	9
5 Flowchart for Parameter Computations.....	18
6 Geometry Depicting Key Scenario Parameters	19
7 Trajectory Plot for Run #1	22
8 Trajectory Plot for Run #2	22
9 Trajectory Plot for Run #3	23
10 Trajectory Plot for Run #4	23
11 Trajectory Plot for Run #5	24
12 Trajectory Plot for Run #6	24
13 Plot of Solution Behavior as a Function of the Number of Iterations	25

LIST OF TABLES

Table		Page
1	Symbols Defined.....	12
2	Run Parameters	20
3	Solution Parameters.....	20

LIST OF SYMBOLS

A	Angle between contact heading and firing platform bearing to contact
B	Bearing of contact relative to own ship at launch
c_{pr}	Constant contact parameters
D_r	Pursuer drift
L_a	Acoustic offset distance (laminar distance)
L_d	Distance traveled by pursuer during dive phase
L_o	Seeker offset distance
L_{sto}	Seeker turn-on distance
o_{pr}	Constant own ship parameters
P_n	Launcher offset, across centerline
P_o	Launcher offset, along centerline
p_{pr}	Constant pursuer parameters
R_a	Range between contact and pursuer at alertment time
R_c	Range of contact
r_c	Turn radius of contact
r_p	Turn radius of pursuer
R_g	Distance traveled by pursuer after launch/prior to turn
S_c	Speed of contact
S_{ca}	Speed of contact after alertment
S_{ct}	Speed of contact in turn
S_p	Speed of pursuer
S_{pd}	Speed of pursuer in dive
S_{ps}	Speed of pursuer in search phase
S_{pt}	Speed of pursuer in turn
t_a	Time at which contact is alerted
t_d	Time at which pursuer starts climb/dive to search depth
t_{dive}	Time in dive phase

LIST OF SYMBOLS (Cont'd)

- t_e Time of pursuer's seeker turn-on
 t_j Time of contact intercept
 t_m Time at start of contact evasive maneuver
 t_{mc} Time at completion of contact evasive maneuver
 t_p Time at start of pursuer turn
 t_{pc} Time at completion of pursuer turn
 t_{srch} Time in search phase
 t_{st} Reaction time of contact

 $\dot{\theta}_c$ Contact turn rate
 θ_c Angle turned through by contact
 θ_{cm} Contact maneuver angle
 θ_p Angle turned through by pursuer

Accession For	
NTIS - CRASH	<input checked="" type="checkbox"/>
DTIC - TAB	<input type="checkbox"/>
Unannounced	<input type="checkbox"/>
Justification	
By _____	
Distribution _____	
Accession Codes	
(Check appropriate)	
Dist	<input type="checkbox"/>
A-1	

A VEHICLE TRAJECTORY METHOD FOR INTERCEPTING AN ALERTED, EVADING CONTACT

1. INTRODUCTION

Various military and nonmilitary applications involve vehicle control systems that include functions such as detection, tracking, classification, localization, vehicle employment (i.e., contact prediction, vehicle setting, and launch), and situation assessment (reference 1). The vehicle employment portion often includes the computational elements for determining the vehicle trajectory that will intercept a designated contact (evader) (reference 2), or place a vehicle (pursuer) in the vicinity of that contact, so that its internal seeker can then operate. The intercept trajectory has always been of primary importance in the delivery of a vehicle to a contact, partly because this path results in the minimum time to impact. Essential parameters associated with this vehicle employment problem are

1. The deflection angle or gyro angle (for a situation where the pursuer is launched from a nontrainable launcher),
2. The time to initiate seeker search (when considering vehicles with internal acquisition and homing systems), and
3. The time to intercept the contact.

The equations that allow for the solution of this problem form the basis for the algorithms required in the vehicle control portion of many systems. Although the equations are nonlinear, rapid solution convergence is required when used in real-time applications. Combat control system weapon-order generation assumes that the contact velocity states remain fixed from vehicle launch to intercept (reference 3). Because advances in contact (evader) sensor capabilities have made it unlikely that a vehicle would remain undetected by the contact until vehicle intercept, advanced concepts should focus on the alerted, evading contact scenario.

2. PROBLEM DEFINITION

The general problem entails determining those parameters that are necessary for employment of a vehicle on an intercept trajectory. For the acoustic torpedo employment problem, this requires determining the straight-line trajectory that results in the laminar point of the weapon intercepting the target. Wherein the standard approach assumes that the contact being pursued maintains a constant course and speed, the approach presented in this report deals with a contact that is alerted and takes evasive action. It is presumed that information, with regard to the expected alertment range of the evader, is available, and that an alertment strategy is selected (references 2 and 4). A key aspect of this formulation is that alertment time is not required to be known *a priori*. The main torpedo parameters to be determined include gyro angle, alertment time, and intercept time. Other parameters such as vehicle run and enable run (run-to-seeker turn-on) are related and are readily computed. Provision is made to account for both evader reaction time and dynamics. Further, this formulation enables a new, more meaningful, error criteria to be introduced that results in the minimum computation time (number of iterations) for particular desired placement accuracy.

3. FORMULATION/SOLUTION OF EQUATIONS

FORMULATION OF EQUATIONS

Figure 1 is an overall block diagram of the system being considered. Sensors obtain information, such as bearing, on the contact or target of interest. This information is used by state estimation techniques (extended Kalman filter, maximum likelihood estimator, etc.) to compute an estimate of the contact's range, course, bearing, and speed. This contact state information, along with those parameters chosen to model the contact's alertment capability and evasion strategy, are also provided to the evading contact intercept computational unit. This unit contains the pursuer-evader weapon order generation (PEWOG) models that determine gyro angle, alertment time, and intercept time; and it is this unit that is the subject of this report.

A functional representation of the evading contact intercept computational unit is shown in figure 2. The basic elements of the unit include a contact model, a pursuer model, an alertment model, an error unit, and a control unit.

The contact model is a mathematical description of the contact trajectory from launch to intercept. The trajectory is segmented into two major components. The first segment is from launch to the alertment point (see figure 3), and the pre-alertment estimates of contact dynamics are used over this segment. The second segment is from alertment to intercept. Because the contact undergoes a delayed (due to reaction time) evasion maneuver during this segment, the propagation of its position to the intercept point is based on both pre-maneuver and post-maneuver dynamics (i.e., evasion strategy) as well as vehicle characteristics.

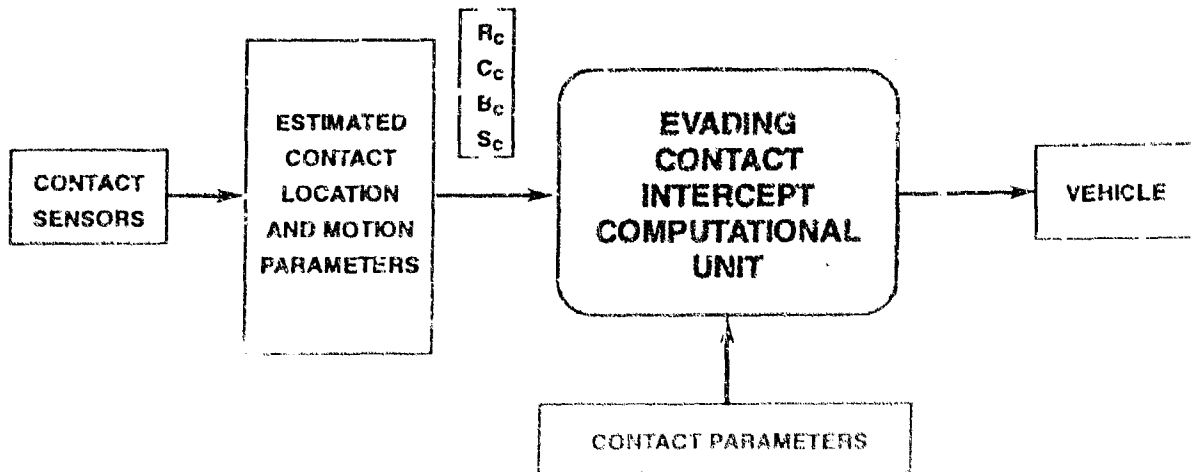


Figure 1. Overall Block Diagram of System

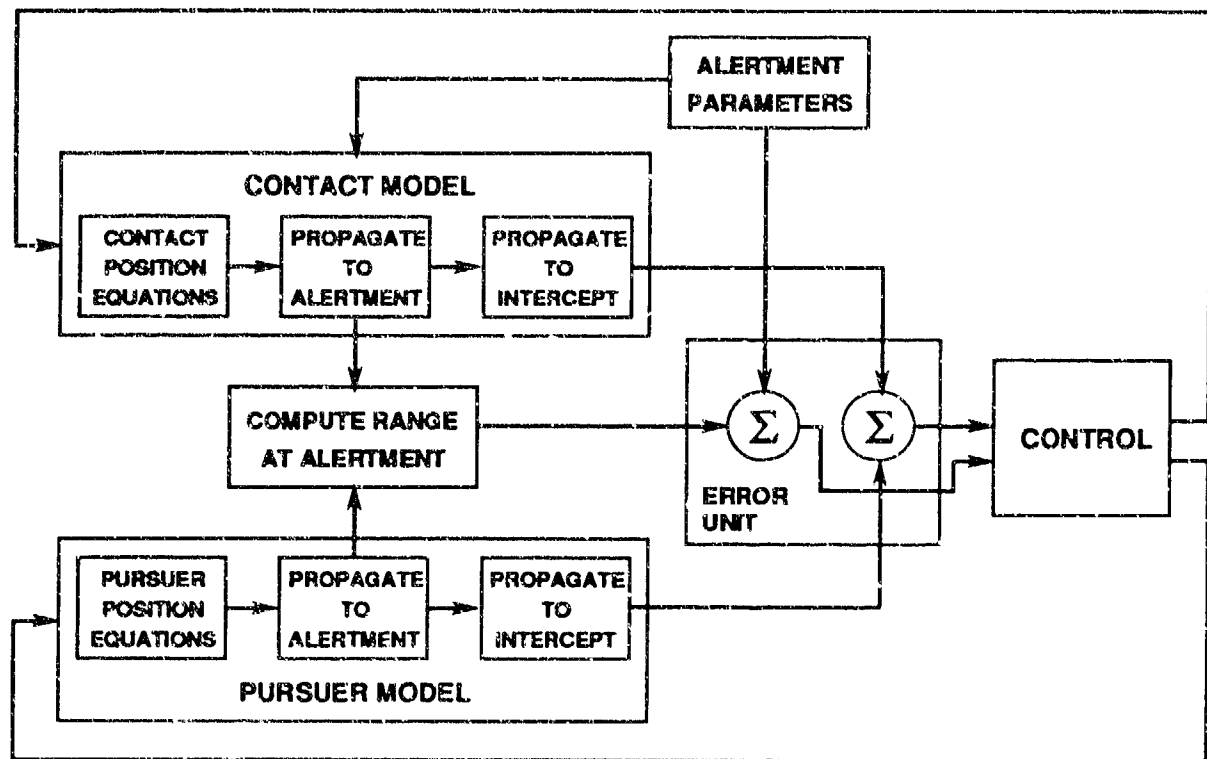


Figure 2. Functional Block Diagram of the Evading Contact Intercept Computational Unit

Similarly, the pursuer's mathematical representation is divided into the same two trajectory components. Because the pursuer can be launched from a platform without trainable tubes and at any depth, the pursuer has to transition to a runout depth and turn to the intercept course. Thus, the propagation of vehicle position over the first segment is a function of weapon settings and characteristics as well as launcher characteristics. During the second segment, alertment to intercept, the pursuer attains optimum search depth and activates its sensor. Pursuer position is propagated over this segment based on weapon settings, characteristics, and sensor parameters.

The alertment model is actually a constraint that is imposed on both the contact and the pursuer trajectories and is a functional representation of the alertment range (contact detection capability), in terms of contact and pursuer prealertment parameters. Thus, at the time of alertment, the range between the contact and pursuer has to equal the alertment range for a valid intercept solution to exist.

Errors are formed between the computed alertment range and the contact detection range, the *across* the line-of-sight positions of contact and pursuer laminar point at intercept, and the *along* the line-of-sight positions of the contact and pursuer laminar point at intercept. These errors are used by the control portion to determine the next set of updates to be fed back for the next computational cycle, if the errors are not less than the convergence criteria.

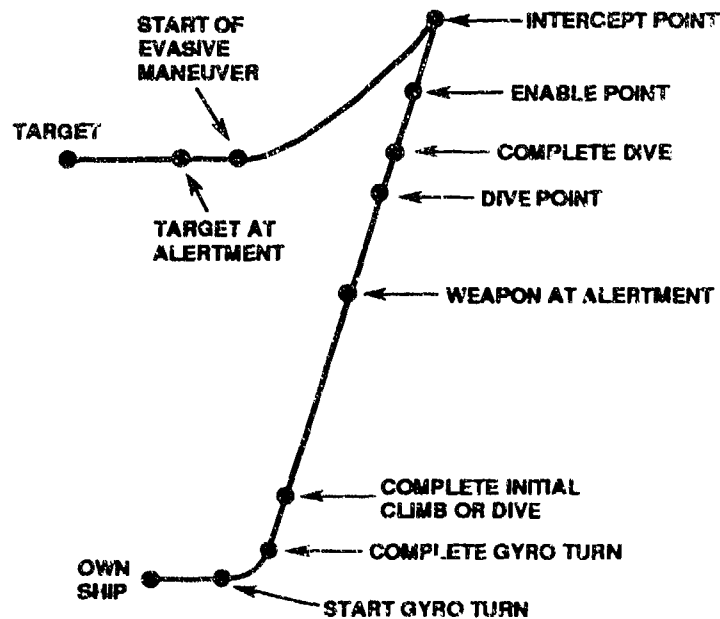


Figure 3. Geometry Depicting Various Points in Vehicle Trajectories

Following the development in reference 2, the equations can be written for the contact, pursuer, and alertment models. These equations take into account

1. A multiple speed pursuer,
2. The ability to specify a seeker turn-on distance or have one computed via specification of an offset distance from the contact,
3. A dive/climb segment to optimum search depth,
4. The drift of the pursuer,
5. Contact reaction time and dynamics, and
6. The situation where the contact is intercepted in its evasive turn.

Definitions of the variables used are given in figures 4a and 4b and the list of symbols on page ii.

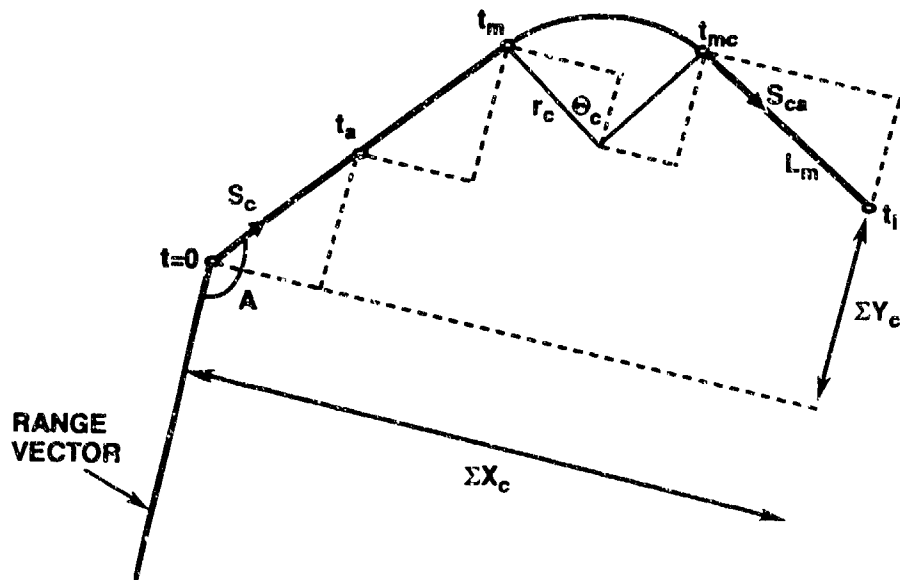


Figure 4a. Contact Track

Contact Model

Figure 4a shows the contact geometry from launch to intercept. Using this diagram, the position equations for the contact are written as

$$\Sigma X_c = -S_c t_a \sin(A) - S_c(t_m - t_a) \sin(A) + r_c \cos(A) - r_c \cos(A - \theta_c) - L_m \sin(A - \theta_c), \quad (1)$$

$$\Sigma Y_c = -S_c t_a \cos(A) - S_c(t_m - t_a) \cos(A) - r_c \sin(A) + r_c \sin(A - \theta_c) - L_m \cos(A - \theta_c), \quad (2)$$

where

$$t_i > t_{mc}, L_m = S_{ca}(t_i - t_{mc}), \text{ and } \theta_c = \theta_{cm},$$

$$t_i < t_{mc}, L_m = 0 \text{ and } \theta_c = \theta_{cdot}(t_i - t_m)$$

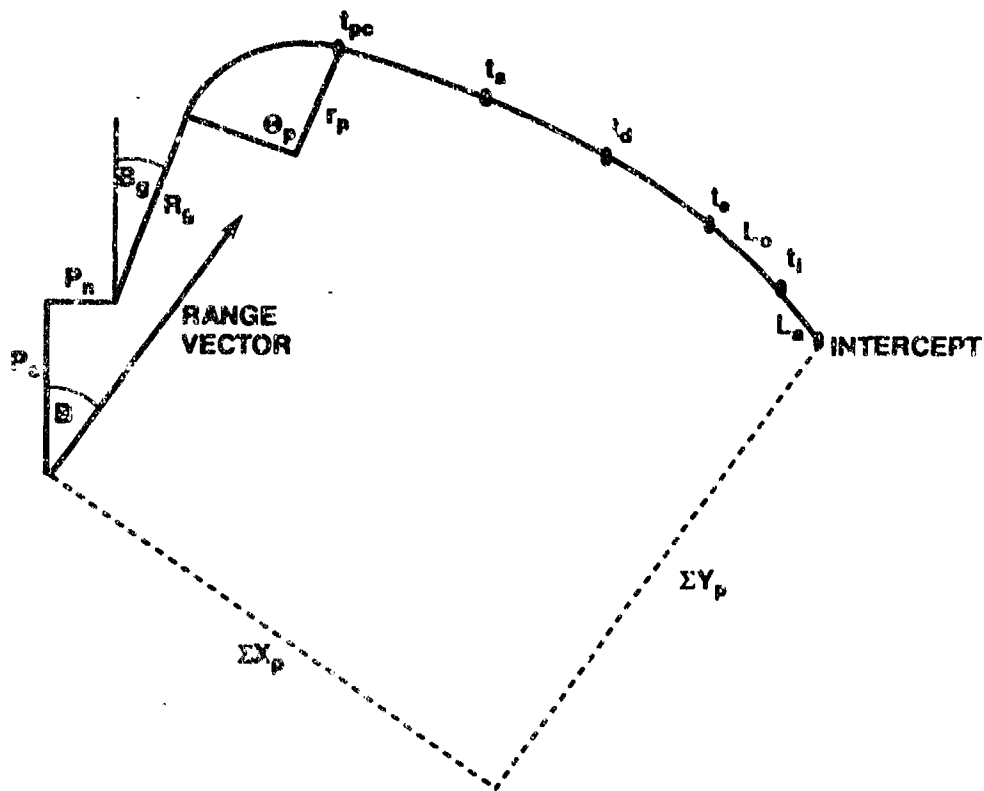


Figure 4b. Pursuer Track

Pursuer Model

Figure 4b shows the pursuer geometry, including launcher parameters, from launch to laminar point intercept of the contact. Using this diagram, the equations for the pursuer can be written as

$$\begin{aligned}
 \Sigma X_p = & P_0 \sin(B) - P_n \cos(B) + R_g \sin(B - B_g) - r_p \cos(B - B_g) + r_p \cos[\theta_p - (B - B_g)] \\
 & - S_p(t_a - t_{pc}) \sin[\theta_p - (B - B_g) + (D_r/2)(t_a - t_{pc})] \\
 & - S_p(t_d - t_a) \sin[\theta_p - (B - B_g) + D_r(t_a - t_{pc}) + (D_r/2)(t_d - t_a)] \\
 & - S_p(t_e - t_d) \sin[\theta_p - (B - B_g) + D_r(t_a - t_{pc}) + D_r(t_d - t_a) + (D_r/2)(t_e - t_d)] \\
 & - S_p(t_i - t_e) \sin[\theta_p - (B - B_g) + D_r(t_a - t_{pc}) + D_r(t_d - t_a) + D_r(t_e - t_d) + (D_r/2)(t_i - t_e)] \\
 & - L_a \sin[\theta_p - (B - B_g) + D_r(t_a - t_{pc}) + D_r(t_d - t_a) + D_r(t_e - t_d) + D_r(t_i - t_e)] .
 \end{aligned} \tag{3}$$

$$\begin{aligned}
\Sigma Y_p = & P_o \cos(B) + P_n \sin(B) + R_g \cos(B - Bg) + r_p \sin(B - Bg) + r_p \sin[\theta_p - (B - Bg)] \\
& + S_p(t_a - t_{pc}) \cos[\theta_p - (B - Bg) + (D_r/2)(t_a - t_{pc})] \\
& + S_p(t_d - t_a) \cos[\theta_p - (B - Bg) + D_r(t_a - t_{pc}) + (D_r/2)(t_d - t_a)] \\
& + S_{pd}(t_e - t_d) \cos[\theta_p - (B - Bg) + D_r(t_a - t_{pc}) + D_r(t_d - t_a) + (D_r/2)(t_e - t_d)] \\
& + S_{ps}(t_i - t_e) \cos[\theta_p - (B - Bg) + D_r(t_a - t_{pc}) + D_r(t_d - t_a) + D_r(t_e - t_d) + (D_r/2)(t_i - t_e)] \\
& + L_a \cos[\theta_p - (B - Bg) + D_r(t_a - t_{pc}) + D_r(t_d - t_a) + D_r(t_e - t_d) + D_r(t_i - t_e)] . \quad (4)
\end{aligned}$$

Alertment Model

The alertment model constrains the range between the contact and pursuer to be equal to the contact detection range at alertment. Using the prealertment contact and pursuer across and along the line-of-sight components, the constraint equation is expressed as

$$\begin{aligned}
R_a^2 = & \{P_o \sin(B) - P_n \cos(B) + R_g \sin(B - Bg) - r_p \cos(B - Bg) + r_p \cos[\theta_p - (B - Bg)] \\
& - S_p(t_a - t_{pc}) \sin[\theta_p - (B - Bg) + (D_r/2)(t_a - t_{pc})] + S_c t_a \sin(A)\}^2 \\
& + \{R_c - S_c t_a \cos(A) - \{P_o \cos(B) + P_n \sin(B) + R_g \cos(B - Bg) + r_p \sin(B - Bg) \\
& + r_p \sin[\theta_p - (B - Bg)] + S_p(t_a - t_{pc}) \cos[\theta_p - (B - Bg) + (D_r/2)(t_a - t_{pc})]\}^2 . \quad (5)
\end{aligned}$$

Error Model

The positional errors are generated from the contact and pursuer across and along the line-of-sight errors at intercept. Equating components yields

$$\Sigma X_c = \Sigma X_p, \text{ or}$$

$$\begin{aligned}
& - S_c t_a \sin(A) - S_c(t_m - t_a) \sin(A) + r_c \cos(A) - r_c \cos(A - \theta_c) - L_m \sin(A - \theta_c) \\
= & P_o \sin(B) - P_n \cos(B) + R_g \sin(B - Bg) - r_p \cos(B - Bg) + r_p \cos[\theta_p - (B - Bg)] \\
& - S_p(t_a - t_{pc}) \sin[\theta_p - (B - Bg) + (D_r/2)(t_a - t_{pc})] \\
& - S_p(t_d - t_a) \sin[\theta_p - (B - Bg) + (D_r/2)(t_d - t_a - 2t_{pc})]
\end{aligned}$$

$$\begin{aligned}
& - S_{pd}(t_e - t_d) \sin[\theta_p - (B - B_g) + (D_r/2)(t_e + t_d - 2t_{pc})] \\
& - S_{ps}(t_i - t_e) \sin[\theta_p - (B - B_g) + (D_r/2)(t_i + t_e - 2t_{pc})] - L_a \sin[\theta_p - (B - B_g) + D_r(t_i - t_{pc})], \quad (6)
\end{aligned}$$

$$\text{and } R_c + \Sigma Y_c = \Sigma Y_p,$$

$$\begin{aligned}
R_c - S_c t_a \cos(A) - S_c(t_m - t_a) \cos(A) - r_c \sin(A) + r_c \sin(A - \theta_c) - L_m \cos(A - \theta_c) \\
= P_o \cos(B) + P_n \sin(B) + R_g \cos(B - B_g) + r_p \sin(B - B_g) + r_p \sin[\theta_p - (B - B_g)] \\
+ S_p(t_a - t_{pc}) \cos[\theta_p - (B - B_g) + (D_r/2)(t_a - t_{pc})] \\
+ S_p(t_d - t_a) \cos[\theta_p - (B - B_g) + (D_r/2)(t_d + t_a - 2t_{pc})] \\
+ S_{pd}(t_e - t_d) \cos[\theta_p - (B - B_g) + (D_r/2)(t_e + t_d - 2t_{pc})] \\
+ S_{ps}(t_i - t_e) \cos[\theta_p - (B - B_g) + (D_r/2)(t_i + t_e - 2t_{pc})] + L_a \cos[\theta_p - (B - B_g) + D_r(t_i - t_{pc})]. \quad (7)
\end{aligned}$$

Using the relationships of table 1 in equations (6) and (7), the positional error equations are,

$$\begin{aligned}
L_{xr} - L_{xc} - r_p \cos(B_1) + r_c \cos(A - \theta_c) + S_c t_a \sin(A) + L_m \sin(A - \theta_c) + r_p \cos(\theta_p - B_1) \\
- S_p \{t_a - [R_g + r_p(\theta_p)]/S_{pt}\} \sin(\theta_p - B_1 + (D_r/2)\{t_a - [R_g + r_p(\theta_p)]/S_{pt}\}) \\
- S_p(t_e - t_a - L_d/S_{pd}) \sin(\theta_p - B_1 + (D_r/2)(t_a + t_e - L_d/S_{pd} - 2\{[R_g + r_p(\theta_p)]/S_{pt}\})) \\
- L_d \sin(\theta_p - B_1 + (D_r/2)(2t_e - L_d/S_{pd} - 2\{[R_g + r_p(\theta_p)]/S_{pt}\})) \\
- S_{ps}(t_i - t_e) \sin(\theta_p - B_1 + (D_r/2)(t_i + t_e - 2\{[R_g + r_p(\theta_p)]/S_{pt}\})) \\
- L_a \sin(\theta_p - B_1 + D_r(t_i - \{[R_g + r_p(\theta_p)]/S_{pt}\})) = 0. \quad (8)
\end{aligned}$$

$$\begin{aligned}
L_{yr} - L_{yc} + r_p \sin(B_1) - r_c \sin(A - \theta_c) + S_c t_a \cos(A) + L_m \cos(A - \theta_c) + r_p \sin(\theta_p - B_1) \\
+ S_p \{t_a - [R_g + r_p(\theta_p)]/S_{pt}\} \cos(\theta_p - B_1 + (D_r/2)\{t_a - [R_g + r_p(\theta_p)]/S_{pt}\}) \\
+ S_p(t_e - t_a - L_d/S_{pd}) \cos(\theta_p - B_1 + (D_r/2)(t_a + t_e - L_d/S_{pd} - 2\{[R_g + r_p(\theta_p)]/S_{pt}\})) \\
+ L_d \cos(\theta_p - B_1 + (D_r/2)(2t_e - L_d/S_{pd} - 2\{[R_g + r_p(\theta_p)]/S_{pt}\}))
\end{aligned}$$

$$\begin{aligned}
& + S_{ps}(t_i - t_e) \cos(\theta_p - B_1 + (D_r/2)\{t_i + t_e - 2[R_g + r_p(\theta_p)/S_{pt}]\}) \\
& + L_a \cos(\theta_p - B_1 + D_r\{t_i - [R_g + r_p(\theta_p)]/S_{pt}\}) = 0.
\end{aligned} \tag{9}$$

In equations (8) and (9) when L_{sto} is selected,

$$t_e = (L_{sto} - L_d)/S_p + L_d/S_{pd},$$

and when L_{sto} is not selected,

$$t_e = t_i - L_o/S_{ps}.$$

Substituting the relationships of table 1 in equation (5) yields the alertment range error equation,

$$\begin{aligned}
& (L_{xr} - r_p \cos(B_1) + r_p \cos(\theta_p - B_1) \\
& - S_p\{t_a - [R_g + r_p(\theta_p)]/S_{pt}\} \sin(\theta_p - B_1 + (D_r/2)\{t_a - [R_g + r_p(\theta_p)]/S_{pt}\}) \\
& + S_c t_a \sin(A))^2 + [R_c - S_c t_a \cos(A) - (L_{yr} + r_p \sin(B_1) + r_p \sin(\theta_p - B_1) \\
& + S_p\{t_a - [R_g + r_p(\theta_p)]/S_{pt}\} \cos(\theta_p - B_1 + (D_r/2)\{t_a - [R_g + r_p(\theta_p)]/S_{pt}\})]^2 - R_a^2 = 0. \tag{10}
\end{aligned}$$

Table 1. Symbols Defined

Symbol	Definition
B_1	$(B - B_g)$
B_2	$(L_o/S_{ps} + L_d/S_{pd})$
L_{xc}	$r_c \cos(A) - S_c(t_{st}) \sin(A)$
L_{xr}	$P_o \sin(B) - P_n \cos(B) + R_g \sin(B - B_g)$
L_{yc}	$R_c - r_c \sin(A) - S_c(t_{st}) \cos(A)$
L_{yr}	$P_o \cos(B) + P_n \sin(B) + R_g \cos(B - B_g)$
t_{dive}	L_d/S_{pd}
$t_e - t_d$	$(L_d)/S_{pd}$
t_m	$t_a + t_{st}$
t_{mc}	$t_a + t_{st} + r_c(\theta_{cm})/S_{ct}$
t_p	R_g/S_{pt}
t_{pc}	$[R_g + r_p(\theta_p)]/S_{pt}$
t_{scrh}	L_o/S_{ps}

Control Model

The errors in equations (8), (9), and (10) are used to generate the control updates required to converge to an intercept solution. The derivation of the control is given in the next section.

SOLUTION OF EQUATIONS

The solution of equations (8) through (10) is now addressed (references 2 and 5). The equations are transcendental in nature and do not lend themselves to solutions in closed form. A numerical solution that exhibits rapid convergence characteristics and accurate estimates is required.

Expressing equations (8), (9), and (10) as general functions of the problem unknowns and performing a Taylor series expansion yields

$$e(t_a, t_i, \theta_p) = e(t_{a_i}, t_{i_i}, \theta_{p_i}) + h \partial e / \partial t_{a_i} + j \partial e / \partial t_{i_i} + k \partial e / \partial \theta_{p_i} + \dots = 0, \quad (11)$$

$$f(t_a, t_i, \theta_p) = f(t_{a_i}, t_{i_i}, \theta_{p_i}) + h \partial f / \partial t_{a_i} + j \partial f / \partial t_{i_i} + k \partial f / \partial \theta_{p_i} + \dots = 0, \quad (12)$$

$$g(t_a, t_i, \theta_p) = g(t_{a_i}, t_{i_i}, \theta_{p_i}) + h \partial g / \partial t_{a_i} + j \partial g / \partial t_{i_i} + k \partial g / \partial \theta_{p_i} + \dots = 0, \quad (13)$$

where

$$\partial e / \partial t_{a_i} = \partial e / \partial t_{a_i} |_{t_a=t_{a_i}, t_i=t_{i_i}, \theta_p=\theta_{p_i}},$$

and

$$t_a = t_{a_i} + h, t_i = t_{i_i} + j, \theta_p = \theta_{p_i} + k.$$

Neglecting the higher order terms, the solution of this linear set of equations is expressed as

$$h = [C_{22}(g_i C_{13} - e_i C_{33}) + C_{23}(e_i C_{32} - g_i C_{12}) + f_i(C_{33} C_{12} - C_{13} C_{32})] / \Delta, \quad (14)$$

$$j = [f_i(C_{31} C_{13} - C_{11} C_{33}) + C_{23}(g_i C_{11} - e_i C_{31}) + C_{21}(e_i C_{33} - g_i C_{13})] / \Delta, \quad (15)$$

$$k = [C_{22}(e_i C_{31} - g_i C_{11}) + f_i(C_{32} C_{11} - C_{12} C_{31}) + C_{21}(g_i C_{12} - e_i C_{32})] / \Delta, \quad (16)$$

and

$$\Delta = C_{11}(C_{22} C_{33} - C_{32} C_{23}) + C_{12}(C_{23} C_{31} - C_{33} C_{21}) + C_{13}(C_{21} C_{32} - C_{31} C_{22}), \quad (17)$$

where e_i , f_i , and g_i are given by equations (8), (9), and (10), respectively

The partial derivatives are

$$\begin{aligned}
 C11 = \partial e / \partial t_a &= r_c (\partial \theta_c / \partial t_a) \sin(A - \theta_c) + S_c \sin(A) \\
 &- L_m (\partial \theta_c / \partial t_a) \cos(A - \theta_c) + (\partial L_m / \partial t_a) \sin(A - \theta_c) \\
 &- S_p (t_a - [R_g + r_p(\theta_p)] / S_{pt}) (D_r / 2) \cos(\theta_p - B_1 + (D_r / 2) \{t_a - [R_g + r_p(\theta_p)] / S_{pt}\}) \\
 &- S_p \sin(\theta_p - B_1 + (D_r / 2) \{t_a - [R_g + r_p(\theta_p)] / S_{pt}\}) \\
 &- S_p (t_e - t_a - L_d / S_{pd}) (D_r / 2) \cos(\theta_p - B_1 + (D_r / 2) \{t_a + t_e - L_d / S_{pd} - 2 \{ [R_g + r_p(\theta_p)] / S_{pt} \}\}) \\
 &+ S_p \sin(\theta_p - B_1 + (D_r / 2) \{t_a + t_e - L_d / S_{pd} - 2 \{ [R_g + r_p(\theta_p)] / S_{pt} \}\}) . \quad (18)
 \end{aligned}$$

$$\begin{aligned}
 C12 = \partial e / \partial t_i &= r_c (\partial \theta_c / \partial t_i) \sin(A - \theta_c) - L_m (\partial \theta_c / \partial t_i) \cos(A - \theta_c) + (\partial L_m / \partial t_i) \sin(A - \theta_c) \\
 &- S_{ps} (t_i - t_e) (D_r / 2) (1 + \partial t_e / \partial t_i) \cos(\theta_p - B_1 + (D_r / 2) \{t_i + t_e - 2 \{ [R_g + r_p(\theta_p)] / S_{pt} \}\}) \\
 &- S_{ps} (1 - \partial t_e / \partial t_i) \sin(\theta_p - B_1 + (D_r / 2) \{t_i + t_e - 2 [R_g + r_p(\theta_p)] / S_{pt}\}) \\
 &- L_a (D_r) \cos(\theta_p - B_1 + (D_r) \{t_i - \{ [R_g + r_p(\theta_p)] / S_{pt} \}\}) \\
 &- S_p (t_e - t_a - L_d / S_{pd}) (D_r / 2) (\partial t_e / \partial t_i) \\
 &\bullet \cos(\theta_p - B_1 + (D_r / 2) \{t_a + t_e - L_d / S_{pd} - 2 \{ [R_g + r_p(\theta_p)] / S_{pt} \}\}) \\
 &- S_p (\partial t_e / \partial t_i) \sin(\theta_p - B_1 + (D_r / 2) \{t_a + t_e - L_d / S_{pd} - 2 \{ [R_g + r_p(\theta_p)] / S_{pt} \}\}) \\
 &- L_d (D_r) (\partial t_e / \partial t_i) \cos(\theta_p - B_1 + (D_r / 2) \{2 t_e - L_d / S_{pd} - 2 \{ [R_g + r_p(\theta_p)] / S_{pt} \}\}) . \quad (19)
 \end{aligned}$$

$$\begin{aligned}
 C13 = \partial e / \partial \theta_p &= -r_p \sin(\theta_p - B_1) \\
 &- S_p (t_a - [R_g + r_p(\theta_p)] / S_{pt}) (1 - D_r r_p / 2 S_{pt}) \cos(\theta_p - B_1 + (D_r / 2) \{t_a - [R_g + r_p(\theta_p)] / S_{pt}\}) \\
 &+ S_p r_p / S_{pt} \sin(\theta_p - B_1 + (D_r / 2) \{t_a - [R_g + r_p(\theta_p)] / S_{pt}\}) \\
 &- S_p (t_e - t_a - L_d / S_{pd}) (1 - D_r r_p / S_{pt})
 \end{aligned}$$

$$\begin{aligned}
& \bullet \cos(\theta_p - B_1 + (D_r/2)(t_a + t_e - L_d/S_{pd} - 2\{[R_g + r_p(\theta_p)]/S_{pt}\})) \\
& - L_d(1 - D_r r_p/S_{pt}) \cos(\theta_p - B_1 + (D_r/2)(2t_e - L_d/S_{pd} - 2\{[R_g + r_p(\theta_p)]/S_{pt}\})) \\
& - S_{ps}(t_i - t_e)(1 - D_r r_p/S_{pt}) \cos(\theta_p - B_1 + (D_r/2)(t_i + t_e - 2\{[R_g + r_p(\theta_p)]/S_{pt}\})) \\
& - L_a(1 - D_r r_p/S_{pt}) \cos(\theta_p - B_1 + (D_r)(t_i - \{[R_g + r_p(\theta_p)]/S_{pt}\})) . \tag{20}
\end{aligned}$$

$$\begin{aligned}
C21 = \partial f/\partial t_a &= r_c(\partial \theta_c/\partial t_a) \cos(A - \theta_c) + S_c \cos(A) \\
& + L_m(\partial \theta_c/\partial t_a) \sin(A - \theta_c) + (\partial L_m/\partial t_a) \cos(A - \theta_c) \\
& - S_p(t_a - [R_g + r_p(\theta_p)]/S_{pt})(D_r/2) \sin(\theta_p - B_1 + (D_r/2)(t_a - [R_g + r_p(\theta_p)]/S_{pt})) \\
& + S_p \cos(\theta_p - B_1 + (D_r/2)(t_a - [R_g + r_p(\theta_p)]/S_{pt})) \\
& - S_p(t_e - t_a - L_d/S_{pd})(D_r/2) \sin(\theta_p - B_1 + (D_r/2)(t_a + t_e - L_d/S_{pd} - 2\{[R_g + r_p(\theta_p)]/S_{pt}\})) \\
& - S_p \cos(\theta_p - B_1 + (D_r/2)(t_a + t_e - L_d/S_{pd} - 2\{[R_g + r_p(\theta_p)]/S_{pt}\})) . \tag{21}
\end{aligned}$$

$$\begin{aligned}
C22 = \partial f/\partial t_i &= r_c(\partial \theta_c/\partial t_i) \cos(A - \theta_c) + L_m(\partial \theta_c/\partial t_i) \sin(A - \theta_c) + (\partial L_m/\partial t_i) \cos(A - \theta_c) \\
& - S_{ps}(t_i - t_e)(D_r/2)(1 + \partial t_e/\partial t_i) \sin(\theta_p - B_1 + (D_r/2)(t_i + t_e - 2\{[R_g + r_p(\theta_p)]/S_{pt}\})) \\
& + S_{ps}(1 - \partial t_e/\partial t_i) \cos(\theta_p - B_1 + (D_r/2)(t_i + t_e - 2\{[R_g + r_p(\theta_p)]/S_{pt}\})) \\
& - L_a(D_r) \sin(\theta_p - B_1 + (D_r)(t_i - \{[R_g + r_p(\theta_p)]/S_{pt}\})) \\
& - S_p(t_e - t_a - L_d/S_{pd})(D_r/2)(\partial t_e/\partial t_i) \sin(\theta_p - B_1 \\
& + (D_r/2)(t_a + t_e - L_d/S_{pd} - 2\{[R_g + r_p(\theta_p)]/S_{pt}\})) \\
& + S_p(\partial t_e/\partial t_i) \cos(\theta_p - B_1 + (D_r/2)(t_a + t_e - L_d/S_{pd} - 2\{[R_g + r_p(\theta_p)]/S_{pt}\})) \\
& - L_d(D_r)(\partial t_e/\partial t_i) \sin(\theta_p - B_1 + (D_r/2)(2t_e - L_d/S_{pd} - 2\{[R_g + r_p(\theta_p)]/S_{pt}\})) . \tag{22}
\end{aligned}$$

$$\begin{aligned}
C23 = \partial f / \partial \theta_p &= r_p \cos(\theta_p - B_1) \\
&- S_p \{ t_a - [R_g + r_p(\theta_p)] / S_{pt} \} (1 - D_r r_p / 2 S_{pt}) \sin(\theta_p - B_1 + (D_r / 2) \{ t_a - [R_g + r_p(\theta_p)] / S_{pt} \}) \\
&- (S_p r_p / S_{pt}) \cos(\theta_p - B_1 + (D_r / 2) \{ t_a - [R_g + r_p(\theta_p)] / S_{pt} \}) - S_p (t_e - t_a - L_d / S_{pd}) (1 - D_r r_p / S_{pt}) \\
&\bullet \sin(\theta_p - B_1 + (D_r / 2) \{ t_a + t_e - L_d / S_{pd} - 2 \{ [R_g + r_p(\theta_p)] / S_{pt} \} \}) \\
&- L_d (1 - D_r r_p / S_{pt}) \sin(\theta_p - B_1 + (D_r / 2) \{ 2 t_e - L_d / S_{pd} - 2 \{ [R_g + r_p(\theta_p)] / S_{pt} \} \}) \\
&- S_{ps} (t_i - t_e) (1 - D_r r_p / S_{pt}) \sin(\theta_p - B_1 + (D_r / 2) \{ t_i + t_e - 2 \{ [R_g + r_p(\theta_p)] / S_{pt} \} \}) \\
&- L_a (1 - D_r r_p / S_{pt}) \sin(\theta_p - B_1 + (D_r / 2) \{ t_i - \{ [R_g + r_p(\theta_p)] / S_{pt} \} \}) . \tag{23}
\end{aligned}$$

$$\begin{aligned}
C31 = \partial g / \partial t_a &= 2 \{ \text{PAR1} \} \left[- S_p \{ t_a - [R_g + r_p(\theta_p)] / S_{pt} \} (D_r / 2) \right. \\
&\bullet \cos(\theta_p - B_1 + (D_r / 2) \{ t_a - [R_g + r_p(\theta_p)] / S_{pt} \}) \\
&- S_p \sin(\theta_p - B_1 + (D_r / 2) \{ t_a - [R_g + r_p(\theta_p)] / S_{pt} \}) + S_c \sin(A) \left. \right] \\
&+ 2 \{ \text{PAR2} \} \left[- S_c \cos(A) - \left(- S_p \{ t_a - [R_g + r_p(\theta_p)] / S_{pt} \} (D_r / 2) \right. \right. \\
&\bullet \sin(\theta_p - B_1 + (D_r / 2) \{ t_a - [R_g + r_p(\theta_p)] / S_{pt} \}) \\
&\left. \left. + S_p \cos(\theta_p - B_1 + (D_r / 2) \{ t_a - [R_g + r_p(\theta_p)] / S_{pt} \}) \right] \right] . \tag{24}
\end{aligned}$$

$$C32 = \partial g / \partial t_i = 0 . \tag{25}$$

$$\begin{aligned}
C33 = \partial g / \partial \theta_p &= 2 \{ \text{PAR1} \} \left(- r_p \sin(\theta_p - B_1) \right. \\
&- S_p \{ t_a - [R_g + r_p(\theta_p)] / S_{pt} \} (1 - D_r r_p / 2 S_{pt}) \cos(\theta_p - B_1 + (D_r / 2) \{ t_a - [R_g + r_p(\theta_p)] / S_{pt} \}) \\
&+ (S_p r_p / S_{pt}) \sin(\theta_p - B_1 + (D_r / 2) \{ t_a - [R_g + r_p(\theta_p)] / S_{pt} \}) \left. \right) + 2 \{ \text{PAR2} \} \left[- \{ r_p \cos(\theta_p - B_1) \right. \\
&- S_p \{ t_a - [R_g + r_p(\theta_p)] / S_{pt} \} (1 - D_r r_p / 2 S_{pt}) \sin(\theta_p - B_1 + (D_r / 2) \{ t_a - [R_g + r_p(\theta_p)] / S_{pt} \}) \\
&\left. - (S_p r_p / S_{pt}) \cos(\theta_p - B_1 + (D_r / 2) \{ t_a - [R_g + r_p(\theta_p)] / S_{pt} \}) \right] \right] . \tag{26}
\end{aligned}$$

where

$$\text{PAR1} = [L_{xr} - r_p \cos(B_1) + r_p \cos(\theta_p - B_1) - S_p \{t_a - [R_g + r_p(\theta_p)]/S_{pt}\} \sin(\theta_p - B_1 + (D_r/2)\{t_a - [R_g + r_p(\theta_p)]/S_{pt}\}) + S_{ct} t_a \sin(A)],$$

$$\text{PAR2} = [R_c - S_{ct} t_a \cos(A) - \{L_{yr} + r_p \sin(B_1) + r_p \sin(\theta_p - B_1) + S_p \{t_a - [R_g + r_p(\theta_p)]/S_{pt}\} \cos(\theta_p - B_1 + (D_r/2)\{t_a - [R_g + r_p(\theta_p)]/S_{pt}\})\}],$$

and for

$$t_i > t_{mc}: L_m = S_{ca}(t_i - t_a - t_{st} - R_c(\theta_{cm})/S_{ct}); \partial L_m / \partial t_a = -S_{ca}, \text{ and } \partial \theta_c / \partial t_a = 0,$$

$$t_i \leq t_{mc}: L_m = 0; \partial L_m / \partial t_a = 0, \text{ and } \partial \theta_c / \partial t_a = -\theta_c \text{dot},$$

and when L_{sto} is selected

$$t_e = (L_{sto} - L_d)/S_p + L_d/S_{pd}; \partial t_e / \partial t_i = 0,$$

and when L_{sto} is not selected

$$t_e = t_i - L_o/S_{ps}; \partial t_e / \partial t_i = 1.$$

Figure 5 is a flowchart of the PEWOG algorithm used to determine the estimates for gyro, alertment time, and intercept time for an evading target scenario. Three logic conditions are included in this block diagram. The first decision point addresses the change in the computations dependent on whether the contact is intercepted in or after completion of the turning maneuver. The second decision point accounts for whether the seeker turn-on (STO) distance is specified or computed based on a seeker offset distance relative to the pursuer position at intercept. The third decision point determines if the computations have converged sufficiently to satisfy specified criteria.

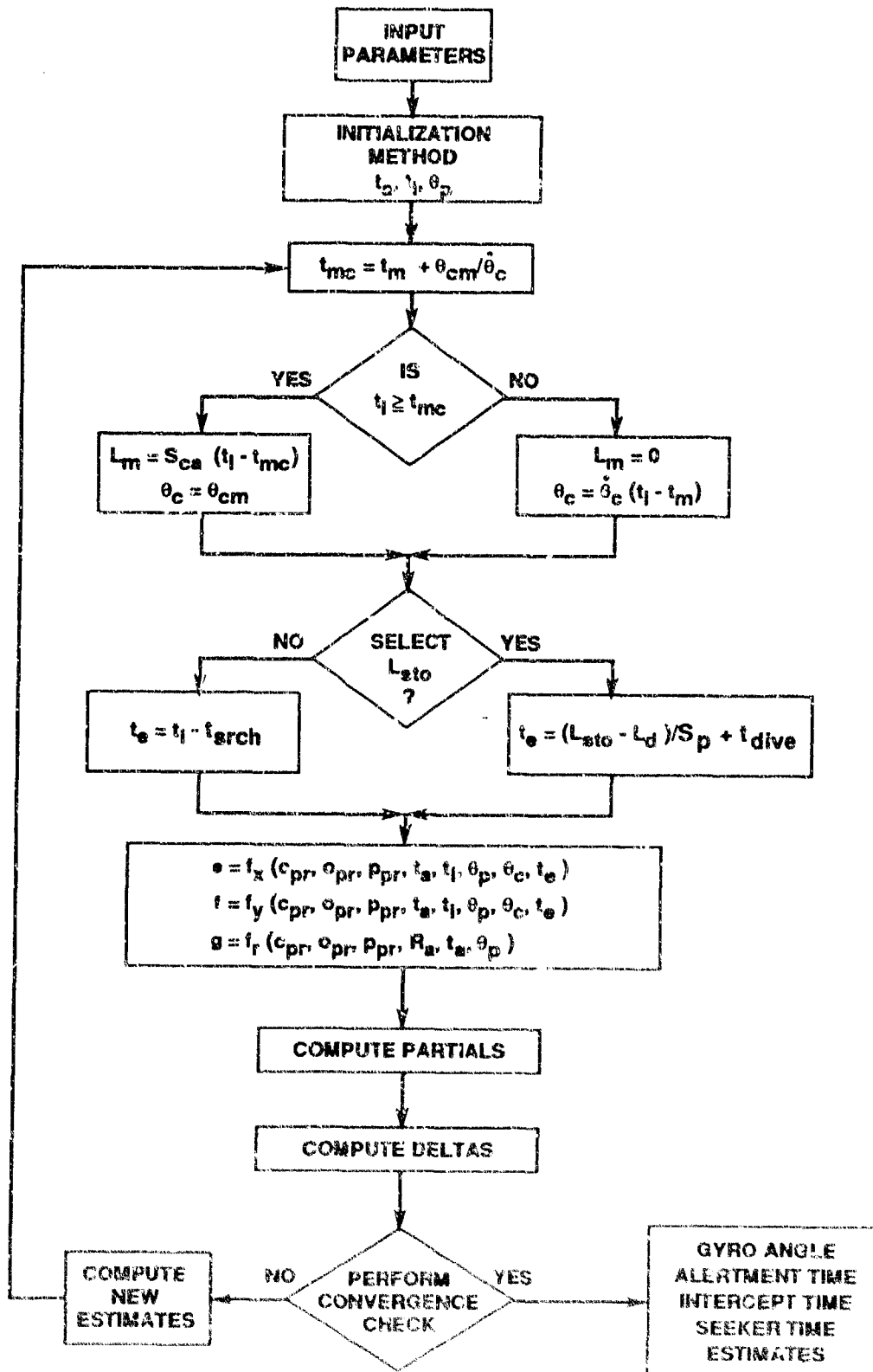


Figure 5. Flowchart for Parameter Computations

4. RESULTS

Figure 6 is a generic geometry for the pursuer/evader problem in which the key problem parameters are indicated. The parameters for each run are specified in table 2 and were used by the PEWOG algorithm to compute a gyro angle, alertment time, and intercept time, as given in table 3. The pursuer vehicle is then launched, in the simulation, and uses the computed gyro angle to establish its course. The simulation continues to propagate all vehicle models until the specified alertment range is reached. At this time, the contact executes its evasion maneuver, taking into account the reaction time and contact dynamics specified. All vehicle models continue to be propagated until intercept. The resulting along and across the track errors are given in table 3. Figures 7 through 12 are the trajectory plots corresponding to the geometries/solutions given in tables 2 and 3.

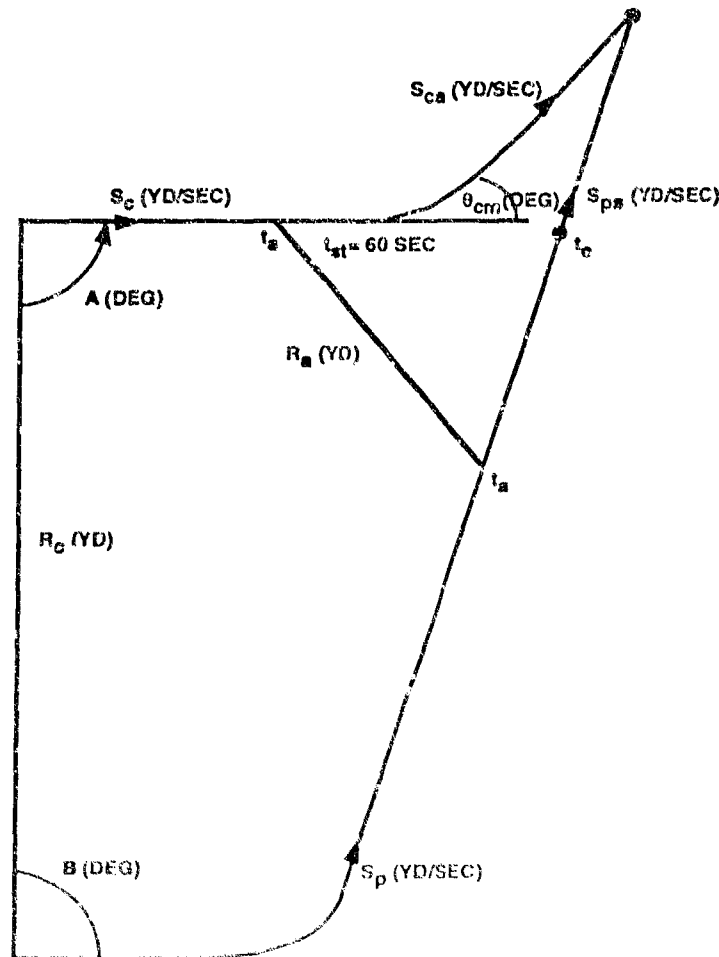


Figure 6. Geometry Depicting Key Scenario Parameters

Table 2. Run Parameters

Run #	B (deg)	A (deg)	Θ_{cm}	S_{ca}/S_c	R_a (kyd)	S_p/S_c	S_{pd}/S_c	S_{ps}/S_c	STO Mode	STO Value
1	-90	90	--	1	4.0	3.1	2.7	2.3	Yes	-1000
2	-90	90	-180	2	4.0	3.1	2.7	2.3	Yes	-1000
3	-90	-90	180	2	4.0	2.3	2.0	2.3	Yes	-1000
4	-90	90	-180	2	3.7	3.1	2.7	2.3	Yes	-1000
5	90	90	45	2	4.8	3.6	3.3	3.1	No	700
6	166	90	45	2	4.5	3.6	3.3	3.1	Yes	-2000

$R_C = 10,000$ yards (Runs #1 through #4); $R_C = 5000$ yards (Runs #5 and #6), $L_a = 1000$ yards, $r_C = 80$ yards, $r_p = 128$ yards, $S_{ct} = S_c$, $S_{pt} = S_p$, $|D_r| = 4.3(10)^{-3}$ deg/sec (all runs)

Note: Run #1 is a contact nonmaneuver case.

Table 3. Solution Parameters

Run	Computer Parameters			Error	
	Gyro (deg)	t_a (sec)	t_i (sec)	e_i (yd)	e_c (yd)
1	-66.7	206.6	324.7	0.24	0.01
2	-73.2	203.6	320.3	0.64	0.06
3	-99.5	295.0	430.2	-0.53	0.01
4	-66.9	215.7	366.1	0.86	0.12
5	103.4	9.5	119.5	0.06	0.01
6	179.3	29.0	129.0	0.13	0.05

Various capabilities of the pursuer evader technique, demonstrated by the run geometries specified in table 2, are summarized as follows:

1. Run #1 treats the case of a constant-course, constant-speed contact and is used as a baseline for comparison. In this run, although the contact is alerted at 4000 yards, no evasive maneuver is performed, thereby, resulting in the solution for a nonmaneuvering contact.

2. Run #2 uses the same initial problem geometry as Run #1; however, when the pursuing vehicle closes to 4000 yards from the contact, alertment occurs and an evasive maneuver is executed, i.e., a 180° change in direction and an increase in speed. The gyro angle computed for Run #2 is larger in amplitude than that of Run #1, reflecting the requirement to intercept a contact moving in the opposite direction from its initial course (or the course of Run #1).

3. In Run #3 the contact portion of the geometry is a mirror image of Run #2. This demonstrates the ability of the algorithm to compute an intercept solution in a different quadrant of the x-y trajectory plane and for a contact with a positive versus negative turn rate, as used in Run #2. Slower pursuer speed parameters were also selected for both the pre-enable and dive portions of the Run #3 pursuer trajectory.

4. Run #4 shows the ability of the model to compute a solution when the point of intercept occurs during the contact evasion turn. The geometry is the same as that of Run #2; however, the alertment range is reduced. This allows the pursuer to get closer to the contact prior to alertment, thereby, resulting in the contact having insufficient time to complete its evasive maneuver before intercept occurs. Comparison of the computed gyro angle for this run with that of Run #1 (nonmaneuvering case) reveals a small difference, as would be expected.

5. The PEWOG algorithm has two modes of operation to determine the weapon seeker turn-on (STO) run distance. Run #5 shows the determination of contact intercept solutions when a STO value is selected as opposed to being computed based on an offset distance from the predicted evading contact's intercept point (as was the case for all other runs). In addition, for Run #5, the initial contact range at launch, alertment range, weapon speeds, and launcher tube (starboard) were selected to be different than those of the previous runs.

6. Run #6 examined the ability of the algorithm to generate a solution for an evading contact that requires a large gyro angle.

The PEWOG algorithm takes into account vehicle drift. Except for Run #4, in which the drift is negative (southern hemisphere), the runs are for a positive drift rate (northern hemisphere). Examination of the along (e_l) and across (e_c) the weapon track errors in table 3 reveals the high degree of accuracy of the algorithm, i.e., all errors are less than 1 yard. Figure 13 is a plot that shows the behavior of the solution parameters as a function of number of iterations of the algorithm. This plot is for Run #2 of table 2, but it is characteristic of the rapid convergence (3 to 4 iterations) exhibited in all runs.

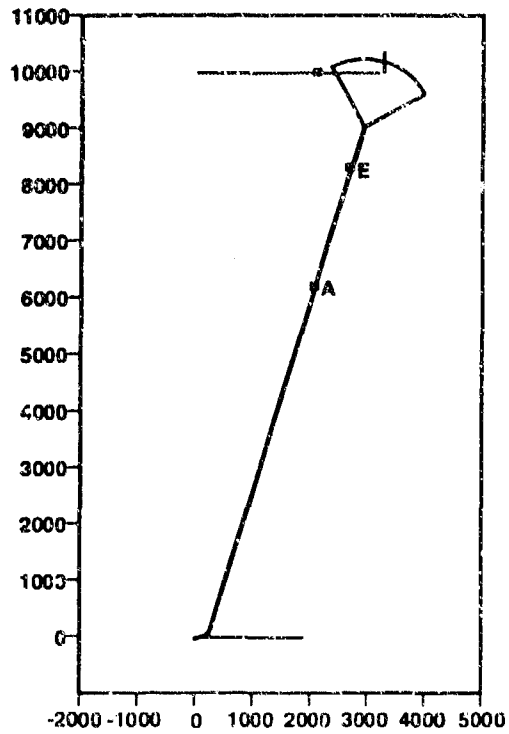


Figure 7. Trajectory Plot for Run #1

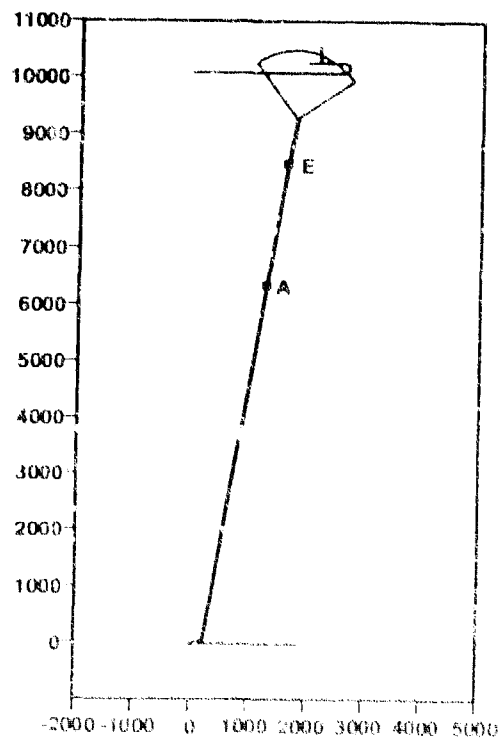


Figure 8. Trajectory Plot for Run #2

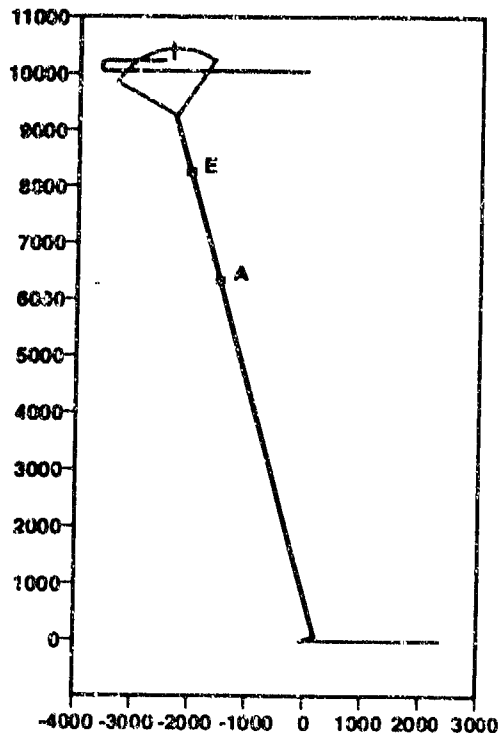


Figure 9. Trajectory Plot for Run #3

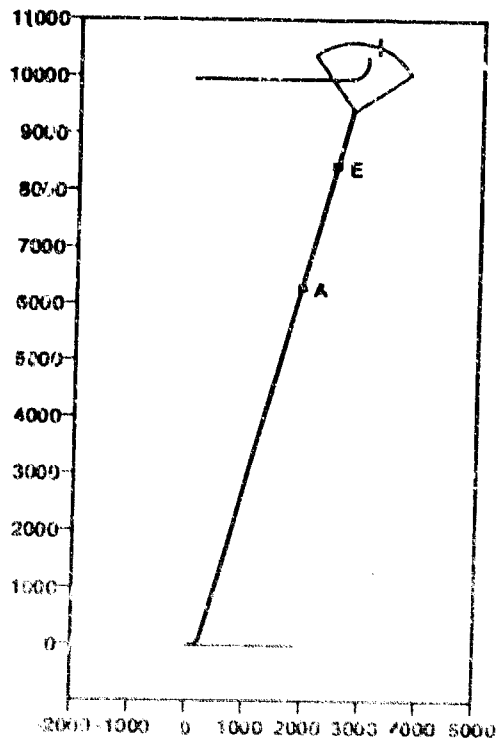


Figure 10. Trajectory Plot for Run #4

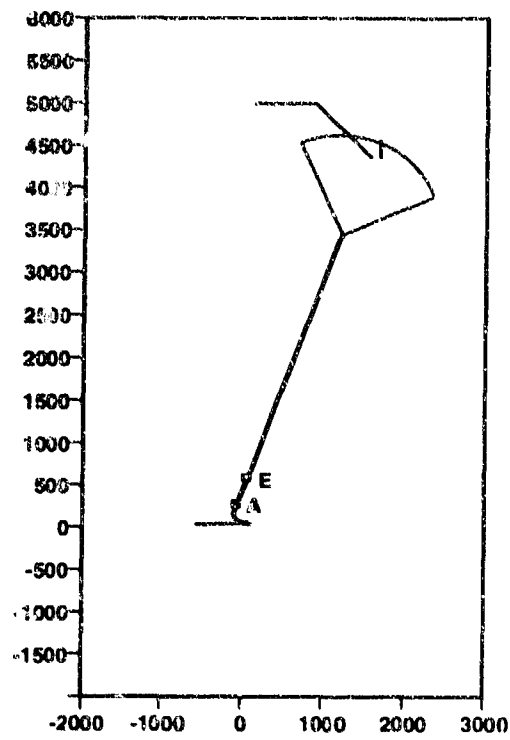


Figure 11. Trajectory Plot for Run #5

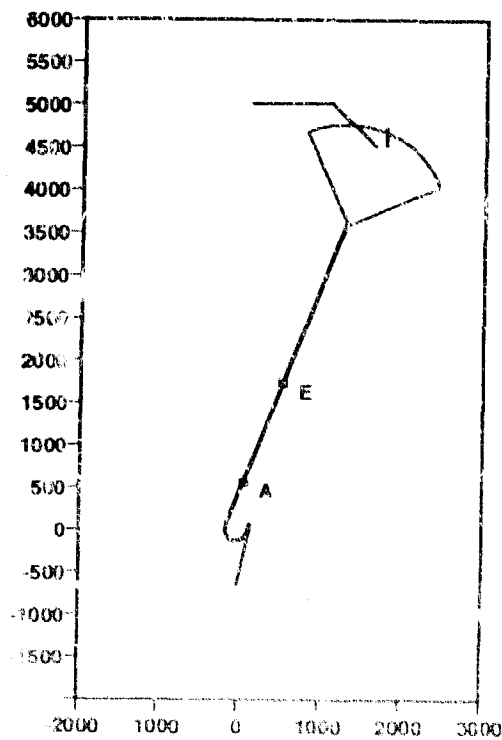


Figure 12. Trajectory Plot for Run #5

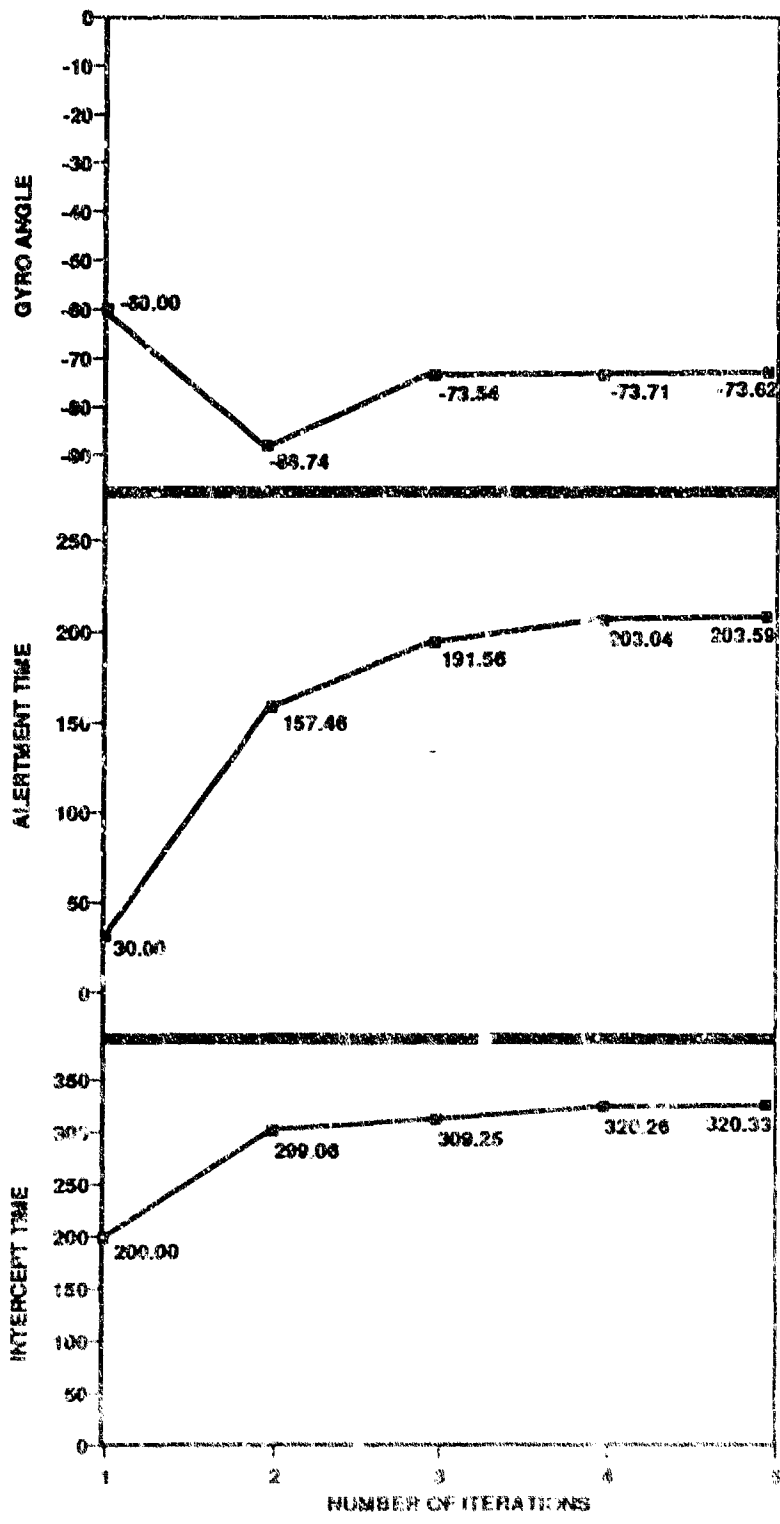


Figure 13. Plot of Solution Behavior as a Function of the Number of Iterations

5. CONCLUSIONS

The intercept method developed in this study relaxes the current intercept requirement of constant contact velocity states for the entire intercept run. This method includes the capability for computing the solution for a pursuer undergoing multiple speed changes, various depth changes, drift, and different sensor activation criteria. In addition, enhancements that account for contact alertment, reaction time, and evasion strategies are added. Intercept by the pursuer can be computed for any point in the contact's trajectory, including during the portion of the trajectory where the contact is turning to an evasion trajectory. Finally, the formulation of the models and the iterative solution technique allow the intercept parameters to be computed faster than real-time (i.e., as fast as the previous nonevasion intercept technique).

A high-fidelity simulation was developed to analyze performance. This computer simulation includes a contact vehicle model, launching platform model, pursuer model, and the PEWOG equations described herein. A large number of pursuer/evader geometries were run, and the accuracy and iteration performance of the technique was examined. An illustrative set of run geometries, along with the associated solution data, are included to illustrate the performance of the technique. The robust behavior of the technique is demonstrated by its ability to generate accurate solutions rapidly. The along (e_l) and across (e_c) the weapon track errors between the contact and the pursuer guidance point, as determined by the simulation at the computed intercept time, are also included along with a plot that demonstrates the rapid convergence of the method

6. REFERENCES

1. Bessacini, A. F., "Advanced Weapon Employment Concept for Combat Control Systems," NUSC Technical Report 6852, Naval Underwater Systems Center, Newport, RI, 1 December 1989 (UNCLASSIFIED).
2. Bessacini, A. F., "Intercept Equations For Alerted, Evading Target Geometries," NUSC Technical Report 6892, Naval Underwater Systems Center, Newport, RI, 15 May 1990 (UNCLASSIFIED).
3. Pinkos, R. F., "Analysis of Weapon Behavior During Corrected Intercept Operation" (U), NUSC Technical Report 4272, Naval Underwater Systems Center, Newport, RI, 15 November 1972 (CONFIDENTIAL).
4. Pereira, D. V., R. F. Pinkos, and A. F. Bessacini, "Weapon Order Generation Equations for Evading Target Aimpoint" (U), NUSC Technical Report 6722, Naval Underwater Systems Center, Newport, RI, September 1988 (CONFIDENTIAL).
5. M. L. James, G. M. Smith, and J. C. Wolford, *Applied Numerical Methods for Digital Computation with FORTRAN and CSMP*, Second Edition, Harper & Row, New York, 1977.

INITIAL DISTRIBUTION LIST

Addressee	No. of Copies
Commander Submarine Force Atlantic	1
Commander Submarine Force Pacific	1
Commander Submarine Development Squadron 12	1
Advanced Research Projects Agency	1
Program Executive Office for Undersea Warfare (ASTO-E)	1
Program Executive Office for Submarines (PMO-425, PMO-4253 -- W. Curles)	2
Submarine Base Pearl Harbor	1
Naval Postgraduate School	1
Naval War College	1
Naval Sea Systems Command (SEA-06U, PMS-393)	2
Defense Technical Information Center	12